

Covalent Chemical Modification of Self-assembled Fluorocarbon Monolayers by Low-energy $\text{CH}_2\text{Br}_2^{+\cdot}$ Ions: a Combined Ion/Surface Scattering and X-ray Photoelectron Spectroscopic Investigation

Nathan Wade, T. Pradeep†, Jianwei Shen and R. Graham Cooks*

Department of Chemistry, Purdue University, West Lafayette, IN 47907, USA

Specific covalent chemical modification at the outermost atomic layers of fluorinated self-assembled monolayers (F-SAMs) on gold is achieved by bombardment with low-energy polyatomic ions (<100 eV). The projectile ion $\text{CH}_2\text{Br}_2^{+\cdot}$ (m/z 172), mass and energy selected using a hybrid ion/surface scattering mass spectrometer and scattered from the F-SAM surface, $\text{CF}_3(\text{CF}_2)_7(\text{CH}_2)_2\text{-S-Au}$, undergoes ion/surface reactions evident from the nature of the scattered ions, CH_2F^+ (m/z 33), CHBrF^+ (m/z 111), and CF_2Br^+ (m/z 129). The chemical transformation of the reactive F-SAM surface was independently monitored by *in situ* chemical sputtering with the projectile Xe^+ . Representative species sputtered from the modified surface include CF_2Br^+ , an indicator of terminal CF_3 to CF_2Br conversion. X-ray photoelectron spectroscopy (XPS) was used to confirm the presence of organic bromine at the surface; Br ($^3\text{P}_{3/2}$) and Br ($^3\text{P}_{1/2}$) peaks were present at binding energies of 182 and 190 eV, respectively. XPS analysis also revealed increased surface modification at higher collision energies in these reactive ion bombardment experiments, as exemplified by the increased hydrocarbon/fluorocarbon peak ratio in the C(1s) region and incorporation of oxygen in the surface seen in the observation of an O(1s) peak. Copyright © 1999 John Wiley & Sons, Ltd.

Received 3 March 1999; Revised 27 March 1999; Accepted 30 March 1999

Specific chemical modification of surfaces has become of growing technological interest for improving the properties of materials. The chemical and physical properties of surfaces can be modified via a large assortment of methods with numerous industrial applications. Simple wet chemical and electrochemical deposition methods are used as a means of modification, as are several gas-phase treatments introduced more recently. In the semiconductor industry, UV irradiation and high-energy ion beam deposition are key elements in the fabrication of integrated circuits and other microelectronic devices.^{1,2} Biomedical implants are coated using chemical vapor deposition and modified using ion grafting procedures to create bioinert or bioactive materials,^{3,4} as needed. Ion beam processing techniques are increasingly of interest for optimizing such properties as hardness and resistance in ceramics⁵ and metals.⁶ Properties of polymeric materials such as wettability, adhesion, and electrical and mechanical performance can be tailored using plasma, X-ray, gamma-ray, UV, ion beam, or electron beam irradiation.^{7–11}

The applications of many polymeric materials depend on their surface reactivity. Therefore, the possibility of

introducing new chemical functionalities at a polymer surface without affecting the bulk properties of the material has proven to be of significant interest. The fundamental types of radiation mentioned above produce modifications in a number of ways. Bonds at the surface may be broken such that molecular fragments are lost, unsaturated groups may be formed or destroyed, and cross-linking may occur as a result of new bonds being formed between different molecules. In addition, reagents delivered to the surface by plasmas,¹² filtered ion beams, or simple molecular exposure can be grafted or adsorbed onto these surfaces.

Ion beam techniques, especially the use of low-energy polyatomic ions, offer several potential advantages for polymer modification. First, numerous reactant ions are readily available, each offering unique reactivity for specific chemical modification. Second, ion beam techniques are valuable in that mass filters can be used to deliver chemically and isotopically pure reactants to a surface.^{13,14} Third, spatial control is available by masking or rastering. Finally, these experiments can be finely controlled since the kinetic energy of the ions, which determines their ability to dissociate, to react, and the extent to which they penetrate the surface can be selected. Most of these mentioned applications have used high-energy beams (>1 keV) in which, generally, chemical modification is the result of physical destruction of a surface. Low-energy ion beams (1–100 eV) offer an alternative route to material modification in that the ion beam itself serves as the chemical reagent allowing modifications to be carefully controlled.^{15–18}

Several different phenomena may occur when ions

*Correspondence to: R. G. Cooks, Department of Chemistry, Purdue University, West Lafayette, IN 47907, USA.

Contract/grant sponsor: The National Science Foundation, USA; Contract/grant number: CHE-9732670.

Contract/grant sponsor: The Fulbright Fellowship.

†Fulbright Scholar, on leave from the Department of Chemistry and Regional Sophisticated Instrumentation Centre, Indian Institute of Technology, Madras 600 036, India.

collide with a surface at low energy (1–100 eV), and the ions scattered from the surface can be studied in an attempt to understand these phenomena.^{19–23} Ion/surface inelastic collisions are well-studied processes whereby the projectile ion picks up internal energy leading to its fragmentation, a process termed surface-induced dissociation.²⁴ Another event, chemical sputtering, involves the ejection of ionic groups derived from the surface through charge exchange.²⁵ The last major process which gives rise to scattered ions is that in which ion/surface reactions occur. These reactions occur between the projectile ion, or its fragments, and specific chemical functional groups on the surface. At collision energies of a few tens of electron volts, bond cleavage and bond formation are thermodynamically accessible. Many of the ion/surface reactions are exothermic, but the collision energy can be used to drive endothermic reactions. Reaction dynamics, however, are dependent on the transfer efficiency of kinetic energy to internal energy,^{26,27} which varies from system to system, and insights into the behaviour of particular systems are obtained by studies performed as a function of collision energy.^{20,28} Chemical reactions are also dependent on the time scale of interaction at the surface.²⁹

Interest in ion/surface reactions has grown not only because of the new reaction types introduced, but because these processes appear to offer viable methods for preparing chemically modified surfaces with high selectivity.^{15,16,30} Unlike high-energy ion beam irradiation, modifications performed through low-energy ion beam irradiation are directly dependent on the chemical nature and reactivity of the projectile, and this dependence allows for selective modification. To understand these processes, mechanisms have been investigated for various ion/surface reactions. Aromatic and heteroaromatic ions have been shown to abstract hydrogen atoms and alkyl groups from hydrocarbon surfaces.^{31–34} In at least some systems the surface functional groups undergo charge exchange with incoming projectile ions, and the fragment ions of these surface-bound radical cations react with the neutralized projectile.³⁵ Kang and co-workers presented a mechanism for Cs⁺ ions picking up Si and H₂O from a Si(111) surface in which neutrals are desorbed from the surface via the collision, then subsequently react with the incoming projectile.^{36,37} Reactive processes at the surfaces of fluorinated self-assembled monolayers^{19,38} have been of interest to this group as well as others. Fluorinated self-assembled monolayer surfaces are noteworthy since they are effective at converting translational energy of the projectiles to internal energy (conversion factor ~ 20%); neutralization of ionic projectiles at the surface is comparatively small due to the high ionization energy of the molecules in the monolayer, and hydrocarbon contamination on the surface is slight under typical vacuum conditions ($\leq 10^{-8}$ Torr). Various projectiles have been shown to abstract fluorine from the F-SAM surface, including C⁺, Si⁺, W⁺, I⁺, and Xe⁺,^{21,39} and several mechanisms have been proposed to explain the transfer of functional groups from this surface to the ion and vice versa,²⁶ including fluorine transfer by oxidative addition²¹ or formation of the fluoronium ion intermediate.⁴⁰

In this communication, the scattering of a mass and energy selected ion beam at low energy from a fluorinated self-assembled monolayer surface is examined with respect to the covalent modification of the outermost portion of the adsorbate monolayer. In an earlier publication,¹⁵ chemical sputtering experiments and static secondary ion mass

spectrometry were used to provide evidence for the occurrence of transhalogenation at the F-SAM surface. In the present study, the polyatomic ion CH₂Br₂⁺ (*m/z* 172) is used as the reactant projectile, and specific covalent attachment of bromine to the surface is sought. Evidence for the modification comes from *in situ* chemical sputtering and, for the first time in this type of study, X-ray photoelectron spectroscopy is used to verify a chemical modification produced by a low-energy polyatomic ion beam. XPS has been used effectively to characterize polymer surfaces⁴¹ as well as self-assembled monolayers.⁴² The presence of covalently bound bromine at the surface is demonstrated.

EXPERIMENTAL

Self-assembled fluorinated alkane thiol monolayers bound to a gold film through a sulfur linkage, CF₃(CF₂)₇(CH₂)₂-S-Au, were used as the surfaces in these experiments. Substrates were prepared by thermal evaporation of chromium and gold onto silicon wafers. The molecular assemblies were constructed by immersing the substrates into dilute (1 mM) ethanol solutions of the fluorinated alkyl thiol. After a few days of exposure, ordered monolayer coverage is achieved. Detailed information concerning the preparation and properties of the surfaces has been provided elsewhere.^{43,44} The surfaces were rinsed with ethanol and dried before being introduced into the high-vacuum scattering chamber.

The ion/surface reactions were performed in a custom-built, hybrid mass spectrometer with geometry BEEQ (B = magnetic sector, E = electric sector, Q = quadrupole mass analyzer), a detailed description of which has been provided.⁴⁵ Briefly, dibromomethane was introduced into the ion source (10^{-5} Torr nominal sample pressure) and ionized by electron impact (70 eV). The resulting ions were accelerated to 2 keV translational energy, and mass and energy selected, respectively, by the magnetic and electrostatic analyzers of a double focusing mass spectrometer. The ion CH₂Br₂⁺ (*m/z* 172) was selected in the ⁷⁹Br₂ isotopic form. This projectile was decelerated to a low translational energy, in the range 20–90 eV, and then allowed to collide with the substrate-covered gold surface which was positioned normal to the ion beam. The surface was housed in a UHV chamber maintained at a nominal pressure of 2×10^{-9} Torr. The primary ion current density was approximately 0.5 nA/cm² with a spot size of about 3 mm². Reaction time for the sample was chosen as three hours, which corresponds to static conditions.

The treated surface was characterized before and after CH₂Br₂⁺ bombardment by chemical sputtering, carried out using 70 eV Xe⁺ (*m/z* 132) as the projectile ion. The sample was rotated so that the primary ion beam was incident at the usual angle of 55° for the chemical sputtering experiment. Scattered ions were collected over a broad range of angles centered at the 90° scattering angle and then analyzed using an electrostatic analyzer, as a kinetic energy to charge filter, and a quadrupole mass analyzer.

After modifications, samples were transferred under argon to a surface analysis chamber where the base pressure was maintained below 10^{-9} Torr. X-ray photoelectron spectra were taken using 70 W electron power with a Mg K α source and an electron spectrometer (Physical Electronics, Eden Prairie, MN, USA) operated with a pass energy of 100 eV in the constant analyzer energy mode. The

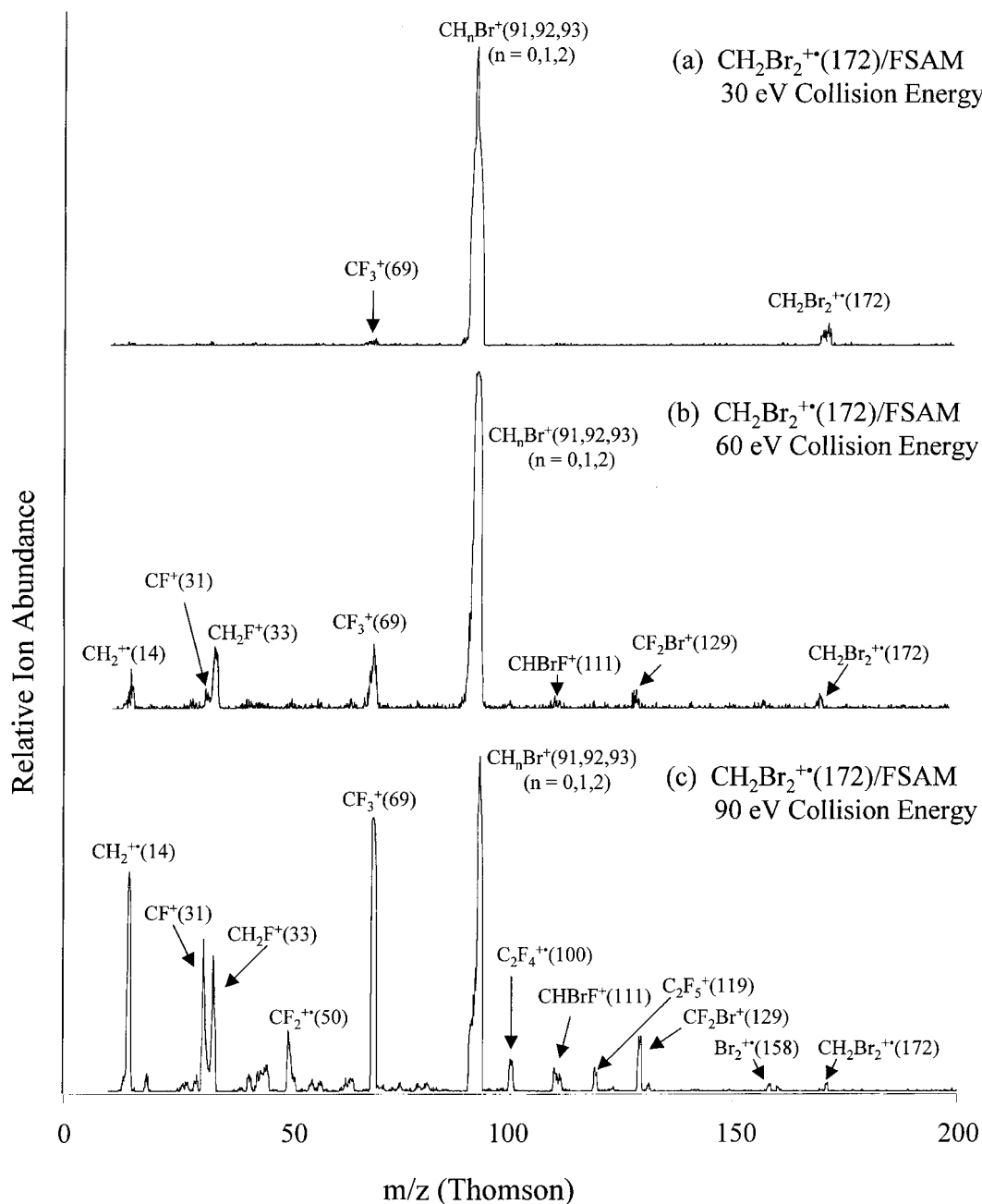


Figure 1. Scattered ion mass spectra recorded upon collision of CH_2Br_2^+ at a fluorocarbon monolayer surface at incident energies (a) 30 eV, (b) 60 eV, and (c) 90 eV.

photoemission angle was kept constant for all experiments. The $\text{Au}(4f_{7/2})$ peak was used as internal reference at a binding energy of 85.0 eV. Peak areas were determined for C(1s), S(2p), Br(3p), and O(1s). Data acquisition times were approximately 15 min for all XPS scans.

RESULTS AND DISCUSSION

The F-SAM surface was treated with the projectile ion CH_2Br_2^+ at energies covering the range 20–90 eV. The goal of this reactive ion scattering experiment was to perform halogen exchange and generate a covalently bound $-\text{CF}_2\text{Br}$ at the surface. Before and after the low-energy ion treatment process, the scattered ion spectra were measured. Figure 1 illustrates the results for the following collision

energies, 30, 60, and 90 eV. The observed scattered ions are formed by a number of different processes. If only a small amount of internal energy is imparted to the ion upon collision, it can in fact scatter from the surface while remaining intact, as evidenced here by the presence of the projectile ion, CH_2Br_2^+ (m/z 172), in the scattered ion spectrum. However, if sufficient translational energy is transferred into internal energy through an inelastic collision, the resulting internally excited projectile ion dissociates to an extent which depends on the energy uptake. Notice that even with a collision energy as low as 30 eV in this system, little of the projectile ion remains intact: surface-induced dissociation yields such product ions as CH_nBr^+ (m/z 90–92, where $n = 0–2$) at this energy and CH_2^+ (m/z 14) at higher energies. The ion Br_2^+ (m/z 158)

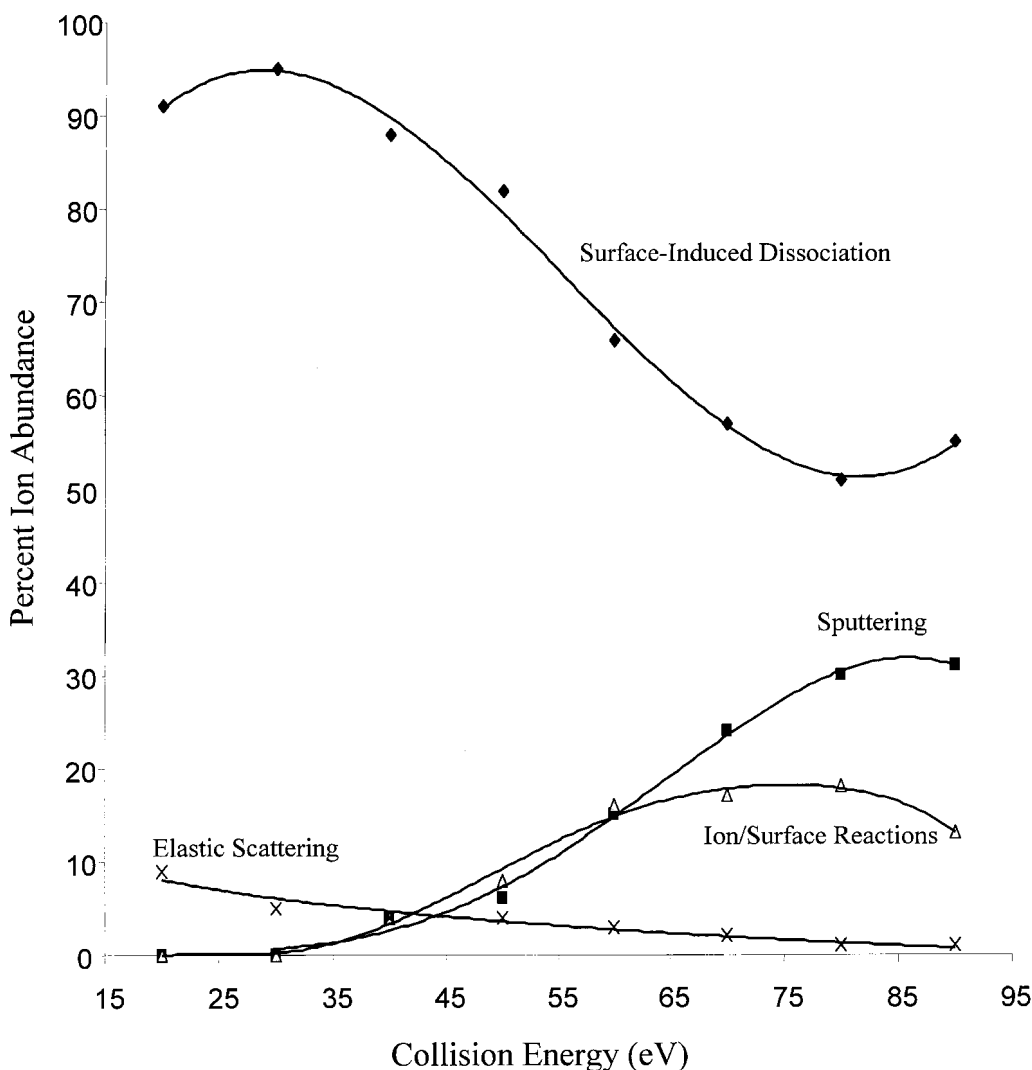


Figure 2. An ERMS plot for the scattered ion products produced upon collision of CH_2Br_2^+ at a fluorocarbon monolayer surface over the collision energy range from 20 to 90 eV.

may also originate via surface-induced dissociation; it is discussed in more detail elsewhere.⁴⁶ Another route to release of ions from the surface is chemical sputtering,²⁵ an event in which the projectile ion undergoes charge exchange with the surface, and in which enough energy is transferred to release the surface-bound species, or their fragments, as gas phase ions. Examples from Fig. 1 include CF^+ (m/z 31), CF_2^+ (m/z 50), CF_3^+ (m/z 69), C_2F_4^+ (m/z 100), and C_2F_5^+ (m/z 119). The fourth and final type of product ions are those generated as the result of ion/surface reactions. Ion/surface reactions can occur by any one of several different proposed mechanisms. In general these reactions include any events in which scattered ions are composed of both the projectile ion, or its fragments, and atoms or groups derived from the surface. In the CH_2Br_2^+ /F-SAM experiments, there is evidence that reactive scattering coincides with the incorporation of bromine into the top portion of the adsorbate monolayer as a consequence of abstraction of atoms from the surface upon collision with a projectile. There is evidence for this in the literature for related systems^{15,16,30} and additional evidence is provided below. In this experiment, fluorine is abstracted from the surface as evidenced by the ion/surface reaction products, CH_2F^+ (m/z 33), CHBrF^+ (m/z 111), and CBrF_2^+ (m/z 129), which have

significant abundance in the 90 eV spectrum (Fig. 1(c)). Figure 2 is an energy-resolved mass spectrometry (ERMS) plot covering the collision energies 20–90 eV. This plot summarizes the collision-energy dependences for the different classes of scattered ions. The relative abundance of elastically scattered ions decreases with collision energy as more internal energy is imparted to the projectile ion yielding greater fragmentation. This behavior has been observed in many other systems. In general, surface-induced dissociation products increase with collision energy; however, as can be seen, at these energies, chemical sputtering and ion/surface reaction processes compete increasingly well in this comparative plot. In this system, ion/surface reactions are most prominent in an energy window of 60–90 eV.

Figure 3 illustrates the Xe^+ chemical sputtering mass spectrum of the F-SAM surface recorded before and after treatment with CH_2Br_2^+ at 60 eV collision energy. The chemical sputtering data of the bombarded sample includes the new ion CF_2Br^+ (m/z 129) along with the ions typical of the unmodified surface. This result suggests that the reactive ion beam bombardment of the surface terminal CF_3 group has caused the chemical transformation to CF_2Br . A similar conclusion was drawn from an earlier study¹⁵ in which

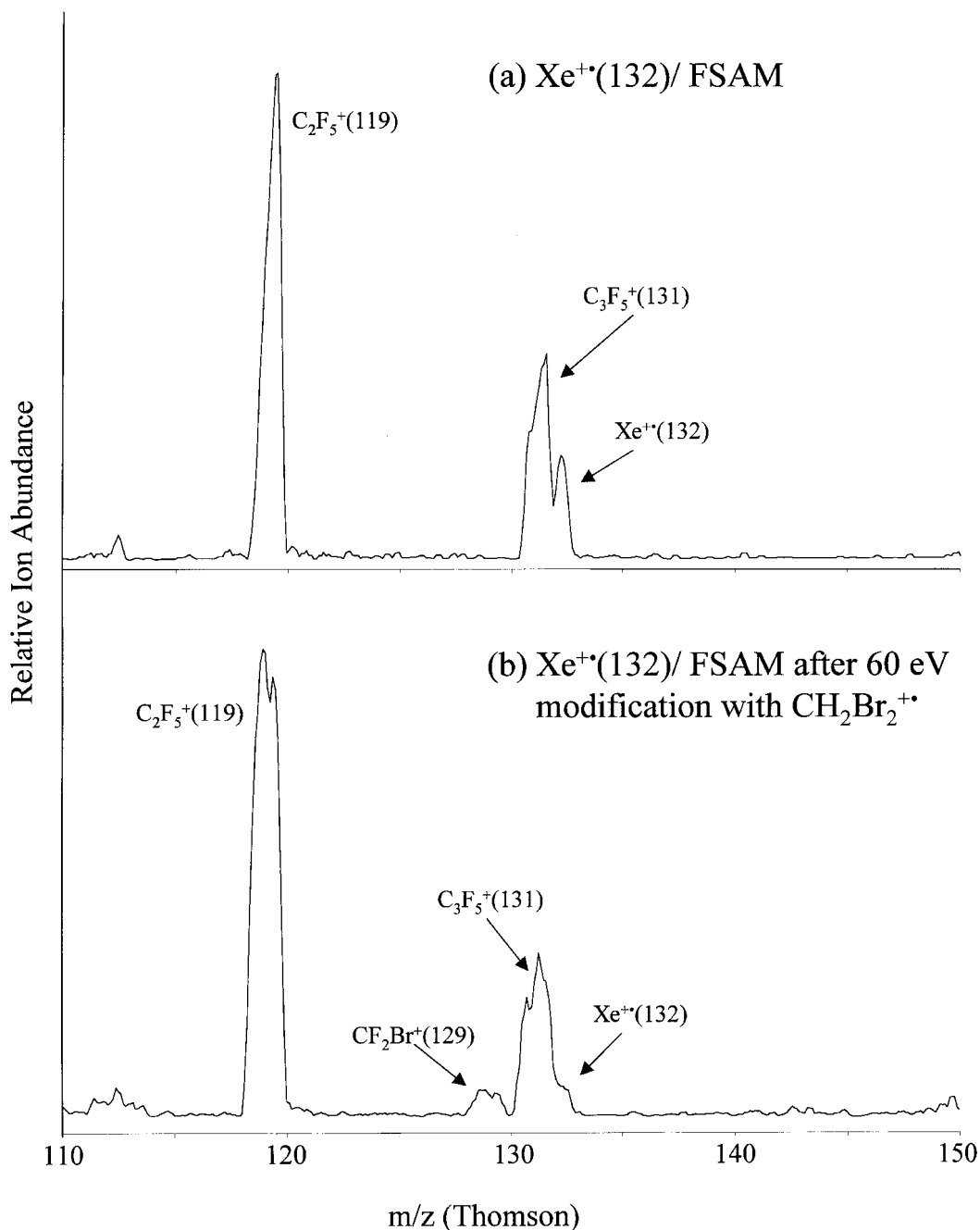


Figure 3. Scattered ion mass spectra recorded upon collision of Xe^+ at 70 eV collision energy with (a) a standard fluorocarbon monolayer surface and (b) a fluorocarbon monolayer surface modified by the projectile CH_2Br_2^+ at 60 eV for a 3 hour time period at approximately 0.5 nA/cm^2 .

secondary ion mass spectrometry was used to examine a surface treated with SiCl_2^+ and likewise CF_2Cl^+ was observed. Chemical sputtering is sensitive to the outermost monolayer of the sample, and bromine modification beyond the terminal layer is indeterminable. Note that Wysocki and co-workers⁴⁷ recently showed that reactivity of low-energy ion beams colliding with a surface is restricted primarily to the terminal functional groups at the surface.

A mechanism previously proposed to account for the transhalogenation reaction suggests that upon collision an intermediate fluoronium ion forms at the surface, and in a concerted fashion the leaving group of the projectile is substituted onto the terminal carbon in exchange for a fluorine.¹⁴ Although there is limited evidence to verify that

this mechanism is correct for this ion/surface reaction, it does agree with evidence that shows that the energy at which modification occurs coincides with that for fluorine abstraction. For example, surface modification was unsuccessfully attempted at 30 eV collision energy, an energy at which the projectile does not show pick-up of fluorine from the surface.

X-ray photoelectron spectroscopy was chosen to provide more direct evidence that bromine was covalently bound to the modified surface. Fluorinated SAM samples which had been bombarded by CH_2Br_2^+ at collision energies of 30, 60, and 90 eV were analyzed. For comparison, the spectrum of an untreated fluorinated SAM was also measured, and Fig. 4 illustrates the $\text{Br}(3\text{P})$ binding energy regions of these

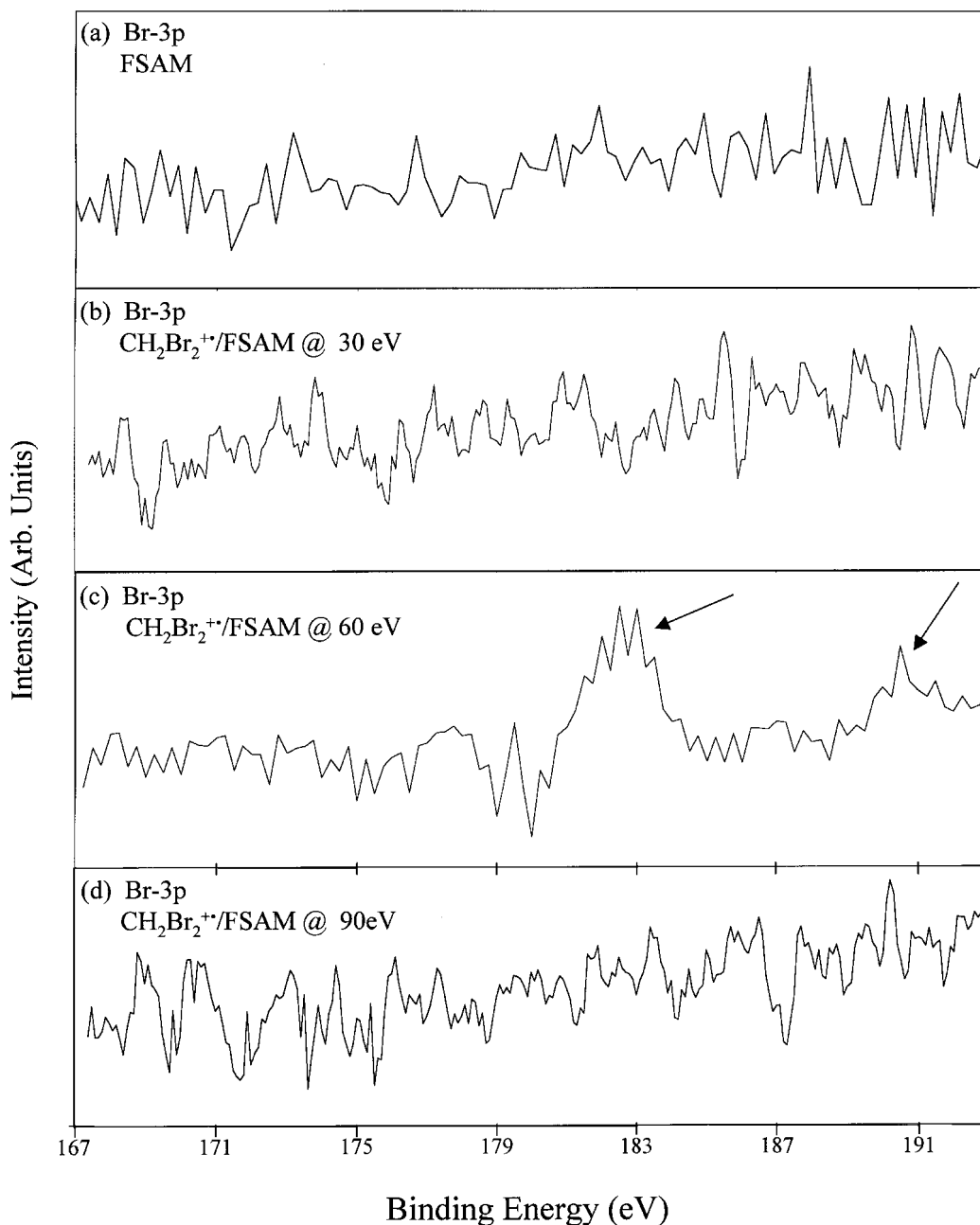


Figure 4. Partial X-ray photoelectron spectra of fluorocarbon monolayer surfaces, illustrating the Br(3p) region: (a) unmodified surface and (b)–(d) modified by the projectile CH_2Br_2^+ using the collision energies shown.

XPS scans. The untreated F-SAM spectra gave no evidence of bromine in the surface region, and neither did the X-ray photoelectron spectra associated with CH_2Br_2^+ delivery at 30 or 90 eV collision energies. At 60 eV collision energy, bromine has been incorporated into the surface, and two peaks representing Br(^3P) are observed in the X-ray photoelectron spectrum: the larger peak, Br($^3\text{P}_{3/2}$), occurs at a binding energy of 182 eV, and the smaller peak, Br($^3\text{P}_{1/2}$), at a binding energy of 190 eV. As expected these peaks are present in an approximately 2:1 intensity ratio, and they correspond in their chemical shift to an alkyl bromide.⁴⁸

Figure 5 shows how the C(1s) region of the X-ray photoelectron spectrum varies with the collision energy used for CH_2Br_2^+ deposition. Previous studies of fluorocarbon and hydrocarbon surfaces yield C(1s) binding energies^{49,50} as follows: R-CF₃ (293–294 eV), R₂-CF₂

(291–292 eV), R₃-CF (290 eV), and R₂-CH₂ (285–286 eV). The peaks in Fig. 5 may certainly correspond to carbons in several different environments, including R-CF₂Br; however, two main peaks dominate the spectra. The smaller peak, at a binding energy of ~286–287 eV, represents hydrocarbon, while the larger peak, at a binding energy of ~291–292 eV, signifies a fluorocarbon. In Fig. 5(a), the peak area ratio of the unmodified F-SAM, C(1s,291)/C(1s,286), is roughly 3:1, consistent with the structure of the monolayer, CF₃(CF₂)₇(CH₂)₂-S-Au. After treatment with 30 eV CH_2Br_2^+ ions, little modification is observed or expected, since the reactive scattering data (Fig. 1(a)) illustrates almost exclusively elastic scattering and surface-induced dissociation. The X-ray photoelectron spectra at 60 and 90 eV collision energies show a distinctive change compared to the standard F-SAM spectrum. At

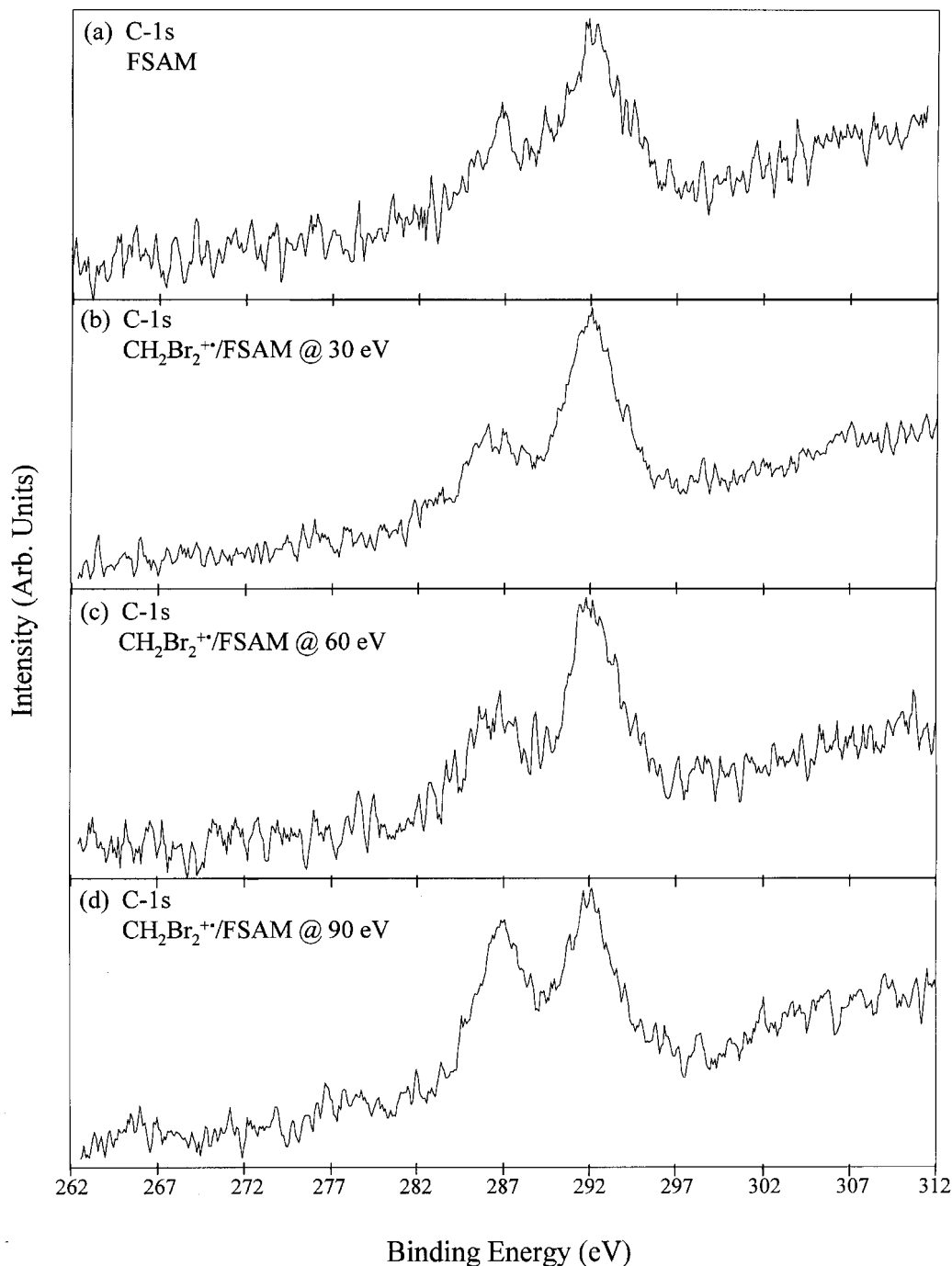


Figure 5. X-ray photoelectron spectra of fluorocarbon monolayer surfaces illustrating the C(1s) region: (a) unmodified surface and (b)–(d) modified with the projectile CH_2Br_2^+ using the collision energies shown.

60 eV collision energy, the ratio between the peaks has changed to approximately 2:1, and at 90 eV collision energy, the peak ratio is approximately 1:1. Hence, at the same energy for which the XPS and chemical sputtering data suggest surface bromination, incorporation of hydrocarbon into the monolayer has also occurred. The hydrocarbon incorporation within the monolayer might arise from adventitious hydrocarbon present within the main chamber. The occurrence of surface C–C cleavage and annealing by hydrocarbons has been observed previously.⁵¹ In the course of ion/surface interactions, atoms and groups are being removed from the surface as bonds are being broken. As the

energy increases, the likelihood that a single collision event in which the projectile reacts with the surface and transfers a group in response to abstraction, as proposed with transhalogenation, becomes more unlikely. Instead, more bonds are broken at the increased energy, and radical sites form at the surface, which are able to recombine with other projectiles. These form unsaturated groups within the monolayer, or react with neighboring chains or material adsorbed at the surface. The last process gives rise to the signals observed at 90 eV.

Water and oxygen are examples of other species which may also be present as contaminants in the vacuum chamber

and, at 90 eV collision energy, oxygen can be shown also to be incorporated into the monolayer. Again a variety of species are present as illustrated by a broad peak spanning binding energies from 531–536 eV, oxygen bonded to carbon has characteristic binding energies, 531–533 eV.^{52,53} This evidence of increased reactivity within the monolayer at 90 eV may explain why selective modification at increased energies is more difficult. Though modifications are occurring to varying degrees within the surface, the monolayer itself is still intact, as evidenced by the S(2p) peaks which occur at a binding energy of 163.5 eV before and after modification. This binding energy corresponds with previous studies of S(2p) for thiols and disulfides on gold.⁵⁴

CONCLUSIONS

Covalent chemical modification of a fluorinated self-assembled monolayer surface has been achieved through bombardment of the surface with low-energy ions as revealed first through in situ chemical sputtering, and now by XPS analysis. The XPS data not only verifies the presence of organic bromine within the surface monolayer, but for higher energy collisions, hydrocarbon and oxygen incorporation into the monolayer is demonstrated. The ability to selectively modify a surface is dependent on the energy of the projectile as well as the reactivity of the system. The success of surface modification by transhalogenation in this system along with others encourages further investigation of this method involving different reactants and surfaces. Quantitation of the degree of modification as a function of the experimental parameters is an objective which remains to be accomplished.

Acknowledgements

This work was supported by the National Science Foundation (CHE-9732670). T.P. acknowledges the award of a Fulbright Fellowship and a Fulbright-Tata travel grant.

REFERENCES

1. C. Ngo and C. Rosilio, *Nucl. Instr. and Meth. B* **131**, 22 (1997).
2. J. S. Williams, *Mat. Sci. E. A* **253**, 8 (1998).
3. D. J. Li and L. Z. Cui, *B. Mater. Sci.* **21**, 445 (1998).
4. J. E. Lemons, *Surf. Coat.* **104**, 135 (1998).
5. W. Bolse, S. D. Peteves and F. W. Saris, *Appl. Phys. A* **58**, 493 (1994).
6. K. Hanamoto, M. Sasaki, T. Miyashita, Y. Kido, Y. Nakayama, Y. Kawamoto, M. Fujiwara and R. Kaigawa, *Nucl. Instr. and Meth. B* **129**, 228 (1997).
7. J. Tian and Q. Xue, *J. Appl. Polym. Sci.* **69**, 435 (1998).
8. O. Tretinnikov, S. Ogata and Y. Ikada, *Polymer* **39**, 6115 (1998).
9. L. J. Matienzo, J. A. Zimmerman and F. D. Egitto, *J. Vac. Sci. Technol. A* **12**, 2662 (1994).
10. W. M. Lau, *Nucl. Instr. and Meth. B* **131**, 341 (1997).
11. F. Arefi, V. Andre, P. Montazer-Rahmati and J. Amouroux, *Pure Appl. Chem.* **64**, 715 (1992).
12. T. G. Vargo, E. J. Bekos, Y. S. Kim, J. P. Ranieri, R. Bellamkonda, P. Aebischer, D. E. Margevich, P. M. Thompson, F. V. Bright and J. A. Gardella, *J. Biomed. Mater. Res.* **29**, 767 (1995).
13. P. Nowak, N. S. McIntyre, D. H. Hunter, I. Bello and W. M. Lau, *Surf. Int. An.* **23**, 873 (1995).
14. O. M. Kuttel, P. Groening, R. G. Agostino and L. Schlapbach, *J. Vac. Sci. Technol. A* **13**, 2848 (1995).
15. T. Pradeep, B. Feng, T. Ast, J. S. Patrick and R. G. Cooks, *J. Am. Soc. Mass Spectrom.* **6**, 187 (1995).
16. J. Shen, V. Grill, C. Evans and R. G. Cooks, *J. Mass Spectrom.* **34**, 354 (1999).
17. E. T. Ada, O. Kornienko and L. Hanley, *J. Phys. Chem. B* **102**, 3959 (1998).
18. J. Q. Sun, I. Bello, S. Bederka and W. M. Lau, *J. Vac. Sci. Technol. A* **14**, 1382 (1996).
19. R. G. Cooks, T. Ast, T. Pradeep and V. Wysocki, *Acc. Chem. Res.* **27**, 316 (1994).
20. T. Ast, Md. A. Mabud and R. G. Cooks, *Int. J. Mass Spectrom. Ion Processes* **82**, 131 (1988).
21. T. Pradeep, T. Ast, R. G. Cooks and B. Feng, *J. Phys. Chem.* **98**, 9301 (1994).
22. W. R. Koppers, M. A. Gleeson, J. Lourenco, T. L. Weeding, J. Los and A. W. Kleyn, *J. Chem. Phys.* **110**, 2588 (1999).
23. C. Mair, T. Fiegele, R. Worgotter, J. H. Futrell and T. D. Mark, *Int. J. Mass Spectrom. Ion Processes* **177**, 105 (1998).
24. Md. A. Mabud, M. J. Dekrey and R. G. Cooks, *Int. J. Mass Spectrom. Ion Processes* **67**, 285 (1985).
25. M. E. Bier, M. Vincenti and R. G. Cooks, *Rapid Commun. Mass Spectrom.* **1**, 92 (1987).
26. T. Pradeep, D. E. Reiderer, Jr., S. H. Hoke, II., T. Ast, R. G. Cooks and M. R. Linford, *J. Am. Chem. Soc.* **116**, 8658 (1994).
27. J. S. Martin, J. N. Greeley, J. R. Morris, B. T. Feranchak and D. C. Jacobs, *J. Chem. Phys.* **100**, 6791 (1994).
28. B. Feng, J. Shen, V. Grill, C. Evans and R. G. Cooks, *J. Am. Chem. Soc.* **120**, 8189 (1998).
29. M. J. Hayward, F. D. Park, L. M. Manzella and S. L. Bernasek, *Int. J. Mass Spectrom.* **148**, 25 (1995).
30. S. A. Miller, H. Luo, X. Jiang, H. W. Rohrs and R. G. Cooks, *Int. J. Mass. Spectrom. Ion. Processes* **160**, 83 (1997).
31. A. Somogyi, T. E. Kane, J. Ding and V. H. Wysocki, *J. Am. Chem. Soc.* **115**, 5275 (1993).
32. M. R. Morris, D. E. Reiderer, Jr., B. E. Winger, R. G. Cooks, T. Ast and C. E. D. Chidsey, *Int. J. Mass Spectrom. Ion Processes* **122**, 181 (1992).
33. B. Winger, R. Julian and R. G. Cooks, *J. Am. Chem. Soc.* **113**, 8967 (1991).
34. E. R. Williams, G. C. Jones, Jr., L. Fang, R. N. Zare, B. J. Garrison and D. W. Brenner, *J. Am. Chem. Soc.* **114**, 3207 (1992).
35. L. M. Phelan, M. J. Hayward, J. C. Flynn and S. L. Bernasek, *J. Phys. Chem. B* **102**, 5667 (1998).
36. M. C. Yang, C. H. Hwang and H. Kang, *J. Chem. Phys.* **107**, 2611 (1997).
37. M. C. Yang, H. W. Lee and H. Kang, *J. Chem. Phys.* **103**, 5149 (1995).
38. K. Vekey, A. Somogyi and V. H. Wysocki, *J. Mass Spectrom.* **30**, 212 (1995).
39. D. E. Riederer, Jr., S. A. Miller, T. Ast and R. G. Cooks, *J. Am. Soc. Mass Spectrom.* **4**, 938 (1993).
40. T. Ast, T. Pradeep, B. Feng and R. G. Cooks, *J. Mass Spectrom.* **31**, 791 (1996).
41. J. X. Chen and J. A. Gardella, *Macromolecules* **31**, 9328 (1998).
42. G. C. Herdt, D. R. Jung and A. W. Czanderna, *J. Adhesion* **60**, 197 (1997).
43. C. E. D. Chidsey, G. Liu, P. Rowntree and G. Scoles, *J. Chem. Phys.* **91**, 4421 (1989).
44. M. Porter, T. Bright, D. Allara and C. E. D. Chidsey, *J. Am. Chem. Soc.* **109**, 3559 (1987).
45. B. Winger, H. Laue, S. Horning, R. Julian, S. Lammert, D. Riederer and R. G. Cooks, *Rev. Sci. Instrum.* **63**, 5613, (1992).
46. T. Pradeep et al., To be Published.
47. C. Gu and V. H. Wysocki, *J. Am. Chem. Soc.* **119**, 12010 (1997).
48. E. Papirer, R. Lacroix, J.-B. Donnet, G. Nanse and P. Fioux, *Carbon* **32**, 1341 (1994).
49. I. H. Loh, M. Klausner, R. F. Baddour and R. E. Cohen, *Polym. Eng. Sci.* **27**, 861 (1987).
50. M.-W. Tsao, C. L. Hoffmann, J. F. Rabolt, H. E. Johnson, D. G. Castner, C. Erdelen and H. Ringsdorf, *Langmuir* **13**, 4317 (1997).
51. E. T. Ada, L. Hanley, S. Etchin, J. Melngailis, W. J. Dressick, M. Chen and J. M. Calvert, *J. Vac. Sci. Technol. B* **13**, 2189 (1995).
52. J. F. Moulder, W. F. Stickle, P. E. Sobol and K. D. Bomben, *Handbook of Photoelectron Spectroscopy*, Perkin-Elmer Corporation, Physical Electronics Division: Eden Prairie, MN 55344 (1992).
53. I. Noh, K. Chittur, S. L. Goodman and J. A. Hubbell, *J. Polym. Sci. A: Polym. Chem.* **35**, 1499 (1997).
54. V. Bindu and T. Pradeep, *Vacuum* **49**, 63 (1998).